Proceedings World Geothermal Congress 2023
Beijing, China, September 15 – 17, 2023

Hydro-thermal Accumulation Mechanism of the Karst Geothermal Reservoir in Heze Burial Uplift of North China

KANG Fengxin[1,2,3*], MA Zhemin[4,5], SHI Qipeng[4,5], ZHENG Tingting[4,5], LIU Xiao[4,5], SUI Haibo[2]

1. College of Earth Science and Engineering, Shandong University of Science and Technology, Qingdao 266590, China

2. 801 Institute of Hydrogeology and Engineering Geology, Shandong Provincial Bureau of Geology and Mineral Resources, Jinan 250014, China

3. School of Water Conservancy and Environment, University of Jinan, Jinan 250022, China

4. Shandong Lunan Geological Engineering Survey Institute, Jining, Shandong, China

5. Shandong Provincial Research Center of Geothermal Energy Exploration and Development, Jining, Shandong, China.

*Corresponding author: Kang Fengxin, kangfengxin@126.com

Keywords: Heze buried uplift geothermal field; karst geothermal reservoir; genetic mechanism; thermal accumulation; water enrichment

ABSTRACT

Karst geothermal reservoirs in buried uplifts in basins are one of the main types of reservoirs used for space heating in China. They are characterized by a wide distribution area, high water temperature, and large amounts of production. They represent an important renewable heat source for clean heating in northern China. Taking the karst geothermal field in the Heze buried uplift as an example, in this paper, the recharge source, migration path, and enrichment mechanism of the karst geothermal water in the geothermal field are revealed through systematic analysis of the geological structure, karst development characteristics, isotope and hydrogeochemical characteristics, the spatial distribution of the geo-temperature field, and the dynamic geothermal water field. The source of the geothermal water is the infiltration of atmospheric precipitation in the bedrock mountains area of Liangshan in the northeast and from Jiaxiang in the east, and mainly accumulates in the compound of interlayered karst and fault zone. According to the characteristics of the heat sources and their transfer and accumulation based on the spatial distribution of the geo-temperature field, a four-source heat accumulation mechanism is proposed. The first source is thermal accumulation of the blanket-shaped terrestrial heat flow conduction. The second source is thermal accumulation of the high thermal conductivity difference in the uplift area. The third source is the belt-shaped convective thermal accumulation in the deep fault zone and the contact zone between the intrusive and soluble rocks. The fourth source is conductive and convective thermal accumulation via deep groundwater circulation. Based on the mechanism of the thermal accumulation and geothermal water enrichment, as well as the controlling factors, such as the water sources, heat sources, and spatial distribution of the geothermal water enrichment reservoir, the metallogenic mode of the karst reservoir in the buried uplift geothermal fields in the basins is a weakly open, convective-conductive, belted-layered type. The metallogenic mode reveals the renewable capacity of the hot water sources and their enrichment, the heat sources and their transfer and accumulation, and the spatial occurrence regularity of the reservoirs.

1. INTRODUCTION

Geothermal systems are relatively independent thermal energy conversion, migration, and storage systems that differ from traditional groundwater systems in terms of the geological environment, hydrological environment, and heat transfer mechanism. Even the geothermal reservoir media are more complex (Muffler, 1979; Rybach et al., 1981; Wright, 1995; Megel et al., 2000; Axelsson, 2008; Wang et al., 2020). Some scholars have systematically studied the law of the geo-temperature field, and after systematic research, it has been concluded that a geothermal anomaly is formed in the uplift area between the two deep depressions. The cap rock is Cenozoic strata, and the lower part is composed of Paleozoic or Middle-Upper Proterozoic carbonate rocks and Archean granite gneiss. In the process of the uniform flow of heat from the deep crust via upward conduction, under the tectonic pattern of the uplift and depressions, because the thermal conductivity of the bedrock is about twice that of the caprock, this difference creates a thermal refraction effect and redistribution of the heat flow, resulting in the bottom heat flow and lateral heat flow entering the high thermal conductivity uplift area, creating localized high geothermal gradients and high heat flow anomalies above the uplift area (Xiong et al., 1982; Chen et al., 1990; Lin et al., 2000; Liu et al., 2005; Feng et al., 2009; Rao et al., 2013; Li et al., 2014; Chang et al., 2016). Some of the boundary faults controlling the uplift area are open faults. Deep hot water upwells along them; and local water-heat convection, convective heat transfer, and conduction transfer occur in the fractured zone and its adjacent karst intervals. The thermal superposition forms a more distinct thermal anomaly. In Well Qianniu 1, which is located in the highest part of the Niutuozhen uplift, the geothermal gradient of the cap rock has been reported to be as high as 11.5°C/100 m, and the temperature at a depth of 500 m was reported to be as high as 72°C, which was the highest in the North China Plain at that time (Chen et al., 1982). The karst thermal reservoir has the characteristics of abundant geothermal resources, good mining conditions, a large water inflow per well, and easy reinjection. It is one of the main thermal reservoirs for the development and utilization of mid-deep geothermal resources (Chen, 1988; Dai et al., 2019). However, due to the heterogeneity of the karst development, the mechanism of the karst geothermal reservoir's heat accumulation and geothermal water enrichment remain to be investigated further (Pang et al., 2015; Wang et al., 2017; Kang, 2018).

The Heze buried uplift geothermal field is located in Heze City, Shandong Province. It is mainly an Ordovician karst thermal reservoir, overlying Cenozoic, Mesozoic, and Late Paleozoic thermal reservoir caprocks. At present, more than 120 karst thermal storage mining wells have been drilled in this reservoir, with a mining volume of about 59,600 m^3/d and water temperatures of 45–75°C, which are mainly used for geothermal heating and bathing. Through the systematic study of the geological structure, isotopic and

hydrogeochemical characteristics, the spatial distribution of the geothermal field, and the dynamic field of the geothermal water, in this study, the recharge source of the karst geothermal water and its migration and enrichment mechanism, as well as the heat source and its transfer and accumulation mechanism were determined. The results of this study provide a reference for the exploration, development, and utilization of the geothermal resources in the karst heat storage geothermal field in the buried uplift in the basin.

2. OVERVIEW OF STUDY AREA

2.1 Geothermal geological conditions

The study area is located in the North China Block, the West Shandong Uplift, the Southwest Shandong buried uplift, the Heze-Yanzhou buried uplift, and the Heze buried uplift, with an area of 6242 km^2. The thermal reservoir is composed of Cambrian-Ordovician carbonate rock, which is mainly gray and brownish-gray limestone. The depth of the thermal reservoir's roof is 700–1300 m, the depth of the bottom is more than 1800 m, and the average thickness is 708 m. The thermal reservoir caprocks are mainly loose Quaternary layers, Neogene sandstone, argillaceous shale, and Carboniferous-Permian sandstone and shale. The caprock gradually thickens from northeast to southwest (Figs. 1 and 2). The geothermal water is from atmospheric precipitation and is mainly supplied by atmospheric precipitation infiltration and deep circulation runoff in the bedrock mountainous areas of Liangshan in the northeast and Jiaxiang in the east. Tianqiao, Juye, Liaokao, and other deep and large faults are developed in the study area, and they communicate with the deep heat sources, forming heat source channels. Secondary faults have developed, and the Ordovician carbonate rocks have experienced strong tectonic movements, forming strong fractured karst development zones, which are the main water source channel.

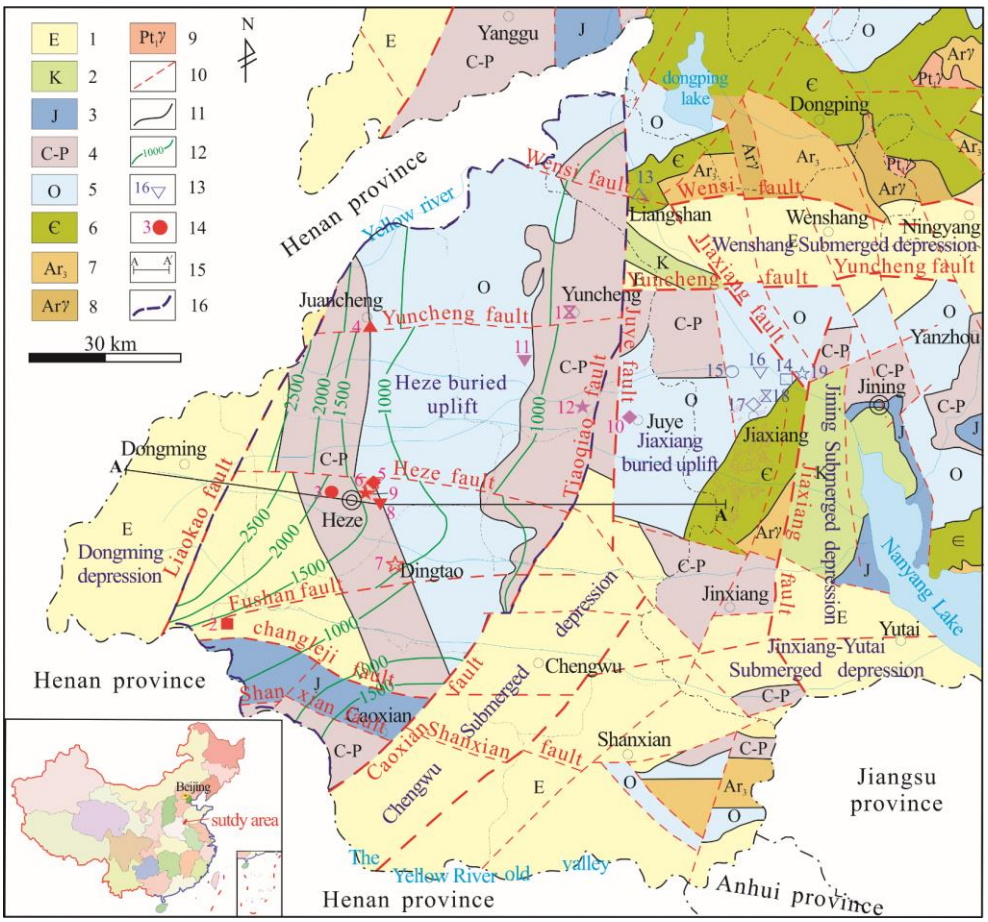

Figure 1: Locations of the karst reservoir and geothermal water sampling points in the Heze buried uplift

1-Paleogene; 2-Cretaceous; 3-Jurassic; 4-Carboniferou-Permian; 5-Ordovician; 6-Cambrian; 7-Neoarchean Taisha Group; 8-Neoarchean intrusive rocks; 9-Paleoproterozoic intrusive rocks; 10-fault; 11-stratagraphic boundary; 12-burial depth contours and depth of Ordovician limestone roof; 13-sampling location of karst cold water; 14-sampling location of geothermal water; 15-section line and its number; 16-distribution area of karst geothermal reservoirs in the Heze buried uplift geothermal field.

2.2 Division of the groundwater flow system in the Heze geothermal field

According to the geological structure, recharge-runoff-discharge-storage of the groundwater, and hydrochemical characteristics, the karst groundwater flow system in the geothermal field in the Heze buried uplift can be divided into three levels (Fig. 2). ① The shallow circulation, open, and unconfined upstream exposed karst areas (open groundwater flow system for short) is located in the upstream recharge area of the karst groundwater flow system. The karst groundwater is recharged via the infiltration of atmospheric precipitation, with strong circulation and alternating characteristics, and it is discharged in the form of decentralized artificial mining. ② A semi-open, semi-confined-confined groundwater flow system (semi-open groundwater flow system for short) is located in the middle reaches of the karst groundwater flow system. It receives lateral runoff recharge from the open water flow system. The runoff

circulates along the fault karst development zone, which is enriched in the fractured karst development area to form a water source. Artificial mining is the main discharge method of karst groundwater. ③ In the downstream buried karst area, deep circulation, weakly open, confined geothermal water flow system (weakly open karst geothermal water flow system for short), a small part of the karst water is blocked by faults and strata and continues to flow along the fault fissure zone to recharge the deep-circulating, weakly open, confined groundwater flow system in the downstream buried karst area, i.e., the weakly open karst geothermal water flow system. During the deep circulation of the runoff, the heat is continuously drawn from the surrounding rocks. Conduction heating by the Earth's heat flow, convection heat accumulation along the thermal conduction fractures, and diversion and heat accumulation in the uplift area occur to form geothermal water, which is mined for geothermal for purposes such as heating and bathing.

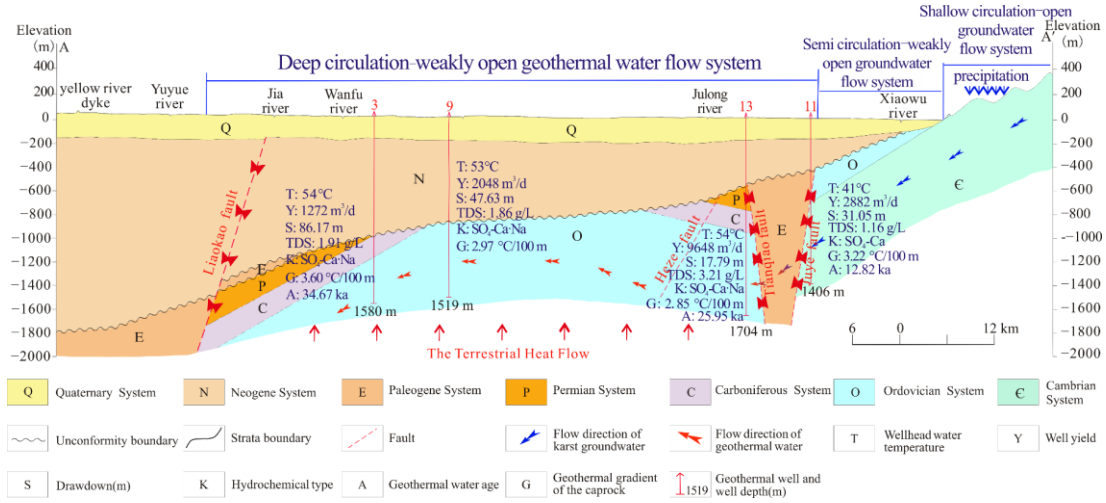

Figure. 2 East-west geothermal geological profile of the Heze buried uplift

3. DATA ACQUISITION AND METHOD

Through systematic analysis of the geological structure, geothermal well and borehole cores, water inflow, temperature measurements, water level, water quality, and isotope data, in this study, the geological structure, karst development characteristics, groundwater dynamic field, and water level dynamics of the geothermal field in the Heze buried uplift, chemical field, and isotopic characteristics were investigated, revealing the sources and migration and enrichment mechanisms of the karst geothermal water. The spatial distribution of the geothermal field was studied, and the heat sources and heat accumulation mechanism of the geothermal field were determined.

The ground temperature was measured using a JHQ-2D series digital logging instrument. The water temperature was the stable water temperature at the wellhead during the pumping test. The water level data used were the measured data from years of monitoring. The water samples were mainly analyzed using an Agilent 51000 inductively coupled plasma optical emission spectrometer (ICP-OES); and an Ion chromatograph was used for bulk analysis. The balance error of the anions and cations was controlled within 3%. The hydrogen and oxygen isotopes and ^{14}C ages were determined by Beta Analytic Inc.

Table 1 shows the bulk analysis results of the karst groundwater and geothermal water from the geothermal field and 19 nearby samples from the Heze buried uplift. The locations of the sampling points are shown in Figure 1. Among them, seven karst groundwater samples were collected in Jiaxiang and Liangshan, and 12 karst reservoir geothermal water samples were collected in the Heze buried uplift. Table 2 presents the data from the drilling, pumping test, temperature measurements, and water level observations for 20 geothermal wells in the karst thermal reservoir; and Table 3 presents the hydrogen, oxygen, and ^{14}C isotope analysis results.

Table 1 Karst geothermal and cold water quality in the study area and nearby area

Sample Number	Sample Location	Sample Type	Temperature (°C)	Analysis items (mg/L)									Hydrochemistry Type
				K^+	Na^+	Ca^{2+}	Mg^{2+}	Cl^-	SO_4^{2-}	HCO_3^-	TDS	pH	
1	YS1	karst geothermal water	48	27.41	256.09	539.77	127.00	270.87	1906.22	177.09	3239.23	7.39	SO_4-Ca
2	CZ1		68	42.58	582.00	475.40	77.80	1499.51	372.23	210.94	1510.83	7.24	Cl-Na·Ca
3	HR1		54	36.06	466.65	578.20	114.30	449.64	1997.63	215.94	1914.63	6.60	SO_4-Ca·Na
4	JZ1		52	38.38	526.90	556.20	138.60	306.23	2341.79	173.79	1959.75	7.47	SO_4-Ca·Na
5	HC1		53	32.50	447.50	524.85	98.76	388.68	1863.90	220.60	1717.40	6.91	SO_4-Ca·Na
6	HJ1		53	35.58	501.30	490.50	102.60	329.56	1943.89	188.67	1647.43	7.46	SO_4-Ca·Na
7	DQ1		58	33.13	503.70	477.30	116.03	452.14	1875.66	234.70	1669.56	7.00	SO_4-Ca·Na
8	HC2		53	37.64	454.40	561.10	110.40	352.40	2055.60	170.92	1855.86	7.42	SO_4-Ca·Na
9	HN1		53.3	32.77	542.86	445.85	95.52	324.66	2062.89	170.16	1504.45	6.92	SO_4-Na·Ca
10	UG1		41	12.15	159.40	320.90	88.21	223.72	954.38	253.98	1164.63	7.26	SO_4-Ca
11	YW1		42	22.21	246.94	603.84	135.3	299.03	2062.65	201.3	3499.89	6.98	SO_4-Ca
12	YR1		54.5	26.95	306.59	497.24	105.48	337.31	1804.33	196.76	3207.07	6.78	SO_4-Ca·Na
13	LG1	karst cold water		3.38	177.78	147.91	58.10	242.46	361.90	351.45	608.57		SO_4·Cl·HCO_3-Na·Ca

14	JT1			3.61	112.31	112.05	55.02	117.23	320.67	313.94	506.36	7.60	SO_4·HCO_3-Ca·Mg·Na
15	JL1			4.12	101.59	167.88	71.61	136.18	458.56	361.82	714.06	7.50	SO_4·HCO_3-Ca·Mg·Na
16	JW1			4.27	129.52	177.34	84.09	147.41	558.16	367.95	789.06	7.40	SO_4·HCO_3-Ca·Mg·Na
17	JS1			4.10	100.50	144.14	83.33	180.17	338.56	358.14	703.06	7.50	SO_4·HCO_3·Cl-Ca·Mg
18	JS2			3.32	111.48	178.95	71.76	185.72	391.82	379.40	742.31	7.70	SO_4·HCO_3·Cl-Ca·Mg
19	JCZ1			3.10	69.00	147.39	53.21	105.05	309.34	324.55	587.13	8.00	SO_4·HCO_3-Ca·Mg

Table 2 Geothermal gradients, water temperatures, yields, and drawdowns of the geothermal wells in the karst reservoir in the Heze buried uplift

Sample Location	Well Depth (m)	Thickness of caprock (m)	Geological age of caprock	Geothermal gradient of caprock (°C/100 m)	Water temperature (°C)	Well yield (m^3/d)	Drawdown (m)
YS1	1810.00	810.00	Q,N,P,C	1.57	47.5	4973.28	18.96
YW1	934.00	656.80	Q,N,	1.90	42.0	3600.00	14.63
YR1	1704.18	936.00	Q,N,P,C	1.98	54.5	9648.00	17.79
YG1	1302.60	950.00	Q,N,P,C	1.78	48.0	5246.40	19.20
YY1	2177.00	750.00	Q,N,P,C	2.39	48.0	7680.00	8.00
JD1	1229.56	1174.00	Q,N,P,C	2.40	55.3	2556.00	7.53
JS1	1503.00	1016.00	Q,N	3.19	53.0	2400.00	11.60
JZ1	1436.20	1078.00	Q,N,C	3.12	52.0	1710.00	90.12
UG1	1406.00	525.00	Q,N	1.38	41.0	2882.40	31.50
HR1	1580.30	962.10	Q,N	3.24	54.0	1272.00	86.17
HC1	1406.18	961.30	Q,N,P,C	3.40	53.0	2106.00	16.86
HJ1	1402.19	973.00	Q,N,P,C	3.39	53.0	2568.96	25.87
HC2	1519.19	979.90	Q,N,P,C	3.22	53.0	2048.64	47.63
HN1	1530.00	1034.96	Q,N,P,C	3.28	53.3	2948.88	25.57
HX1	1200.00	1050.00	Q,N,P,C	3.49	52.0	1458.96	35.31
DQ1	1230.26	1032.25	Q,N,P,C	4.01	58.0	1731.84	3.16
DM1	1400.14	1067.30	Q,N,P,C	3.29	55.0	1611.12	10.75
CM1	2000.00	1850.00	Q,N,J,P,C	2.69	/	/	/
CZ1	1969.98	1344.50	Q,N,E	4.20	68.0	2163.36	33.43

Note: / means no temperature measurement and water pumping test data are available.

Table 3 Isotopic compositions of the geothermal water from the Heze buried uplift geothermal field

Sample Location	δD (SMOW, ‰)	δO^{18} (SMOW, ‰)	^{14}C apparent age (ka)	^{14}C correct age (ka)
HN1	−63.92	−9.39	/	//
CZ1	−73.20	−9.96	34.45	24.73
DQ1	−64.85	−6.40	/	/
HR1	−66.63	−7.03	39.17	35.81
HX1	−70.10	−8.70	/	/
YS1	−71.00	−9.10	37.35	29.81
UG1	/	/	17.720±0.910	12.82
YR1	/	/	31.46	25.95
YW1	/	/	33.23	26.20
JS1	/	/	37.92	31.45
DM1	/	/	38.79	31.67

Note: / means not detected.

4. RESULTS AND ANALYSIS

4.1 Karst development

The fractured karst serves as the deep geothermal water circulation migration channel and enrichment storage space. In the long process of tectonic evolution, the development of deep karst forms in the geothermal field in the Heze buried uplift was controlled by factors such as the structure, burial conditions, depositional environment, and dynamic groundwater field.

4.1.1 Control of structure on karst development

The secondary fault structures near the deep faults such as the Liaokao, Heze, Tianqiao, and Wensi faults are relatively well-developed, and the carbonate rocks have undergone strong tectonic movement, weathering erosion, and multi-stage dissolution, forming a strong fractured karst development zone with a large water abundance. The fissure karst rate is generally about 3%, in the

developed section of the fractured karst, but the fractured karst rate can reach 6% to 54%. The fractured karst development depth is generally 500 to 1800 m, and the cumulative thickness of the aquifer is 18.4 to 133.0 m (Fig. 3). The CZ1 geothermal well is located near the Liaokao and Fushan faults. The fractured karst development depth is 1650–1800 m; the cumulative aquifer thickness is 87.57 m; the single well water inflow is 2386 m^3/d; and the drawdown is 44.81 m, with a large water abundance. Geothermal well YR1 in Yuncheng, is located in a compound site at the intersection of the Tianqiao secondary fault, Zhaohedong fault, and Zhaohe anticline axis. Due to multiple periods of tectonic movement, the fractured karst is very well-developed, and the development depth is 1022.98–1446.30 m. The cumulative thickness of the aquifer is 102.4 m; the water inflow volume of a single well is 9648 m^3/d; the drawdown is only 10.35 m; and the water abundance is extremely high (Fig. 4).

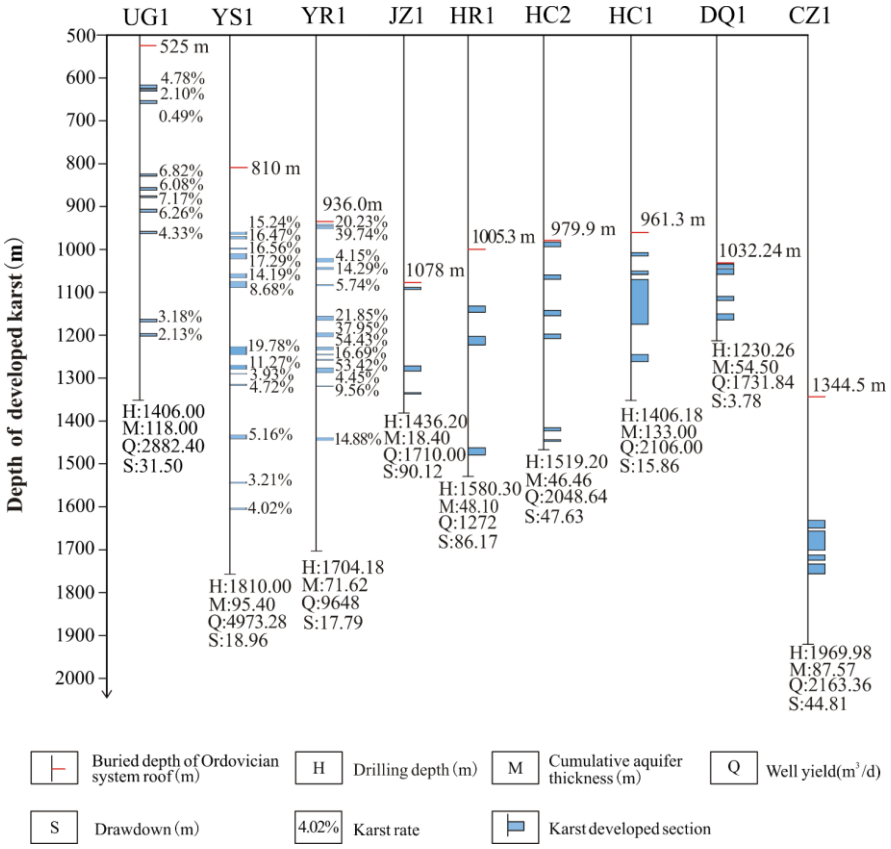

Figure. 3 Karstification development depth in the Heze buried uplift

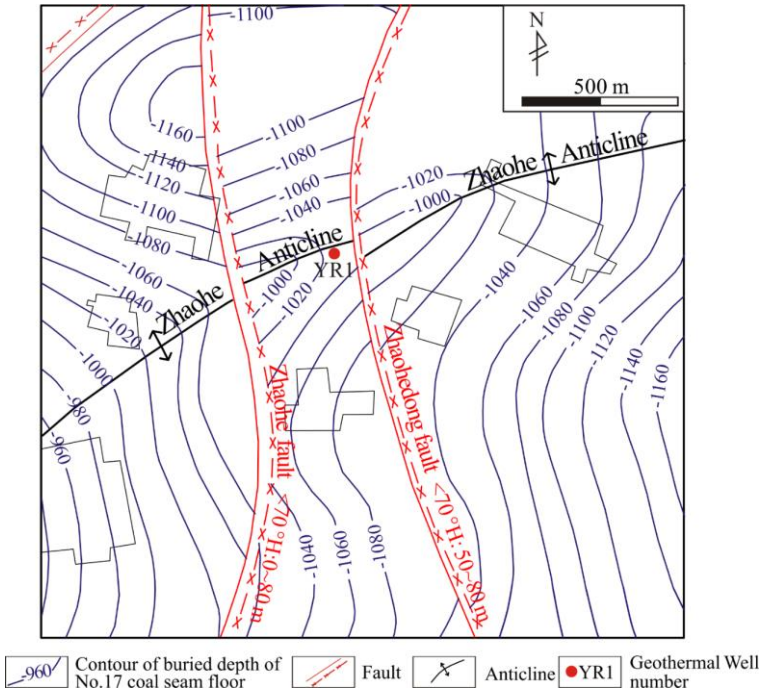

Figure. 4 Structural location of geothermal well YR1 in Yuncheng

4.1.2 Characteristics of interlayer karst development

In the study area, the longer the Ordovician strata have been exposed, the longer the weathering and leaching time, which is favorable for the development of karst structures in the Ordovician reservoir. The geothermal wells that encounter the Neogene caprocks contain the most fractured karst. The geothermal wells that encounter the Carboniferous-Permian caprocks, contain the second most fractured karst, and the thicker the Carboniferous-Permian is, the slower the groundwater flow is. The dissolution ability of the water is basically lost, and the karstification is dominated by precipitation and filling, which makes the ancient karst pores tighter (Jiang, 2014) and the development of fractured karst weaker in the Ordovician. The geothermal well hole in Yuncheng, is 936 m deep. It contains a thermal reservoir of Ordovician carbonate rocks, which overlies the Neogene strata, and it lacks Carboniferous-Permian, Jurassic, and Paleogene strata. The sedimentary gap is as long as 0.41 Ga (Chen et al., 1985), that is, the Ordovician carbonate strata experienced a weathering and leaching period of up to 0.41 Ga before being covered by the Neogene strata. The Ordovician thermal reservoir experienced multiple karstification processes such as scouring, dissolution, and weathering, forming rich interlayered fissured karst, providing good channels for the occurrence and migration of groundwater and a strong water-rich area of geothermal water. The thermal storage roof in this well has a burial depth of 650 m. During the drilling process, in the 702.83–703.43 m interval, the phenomena of drill falling and mud leakage occurred, indicating karst development in this section. Based on the pumping test, the water inflow volume of this well is 3600 m^3/d, with a drawdown of 14.63 m, and the water abundance is high.

4.1.3 Karst development and groundwater dynamics

Groundwater dynamics are a necessary condition for karst development. The farther the geothermal water is from the recharge area, the worse the hydrodynamic conditions are, the weaker the development of the fissured karst is, and the poorer the water abundance is (Fig. 5). Yuncheng is close to the recharge area, the geothermal water circulation runoff speed is fast, and the development of fractured karst is strong. The depth of the fractured karst development in the geothermal wells is 900–1600 m, the cumulative thickness of the aquifer is 95.4 m, and the water inflow volume is 4793 m^3/d. with a drawdown of 18.96 m. The thermal reservoir has abundant water. The geothermal wells HR1 and HC2 in Heze are far from the recharge area, the hydrodynamic conditions are poor, the development of fissured karst is weak, and the geothermal water is in a stagnant state. The development depths of the fissured karst in the geothermal wells are 1180.4–1269.6 m and 983.9–1498.85 m, the cumulative aquifer thicknesses are 48.1 m and 46.46 m, the water inflow volumes are 1272 m^3/d and 2048 m^3/d, and the drawdowns are 86.17 m and 47.63 m, respectively. The thermal reservoir has a poor water abundance.

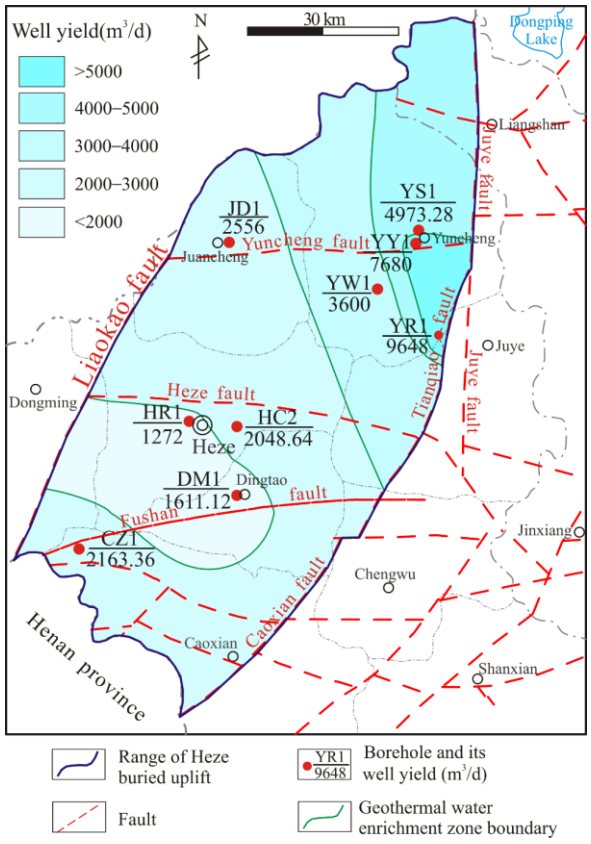

Figure. 5 Single well yield zonation in the karst reservoir in the Heze buried uplift

4.1.4 Karst geothermal water circulation depth

The depth of geothermal water circulation is a very important parameter for studying geothermal fields, and it plays an important role in understanding the genetic types of the geothermal water and the formation mechanism of geothermal fields (Wang et al., 1990; Luo et al., 2017). In this study, the SiO_2 temperature scale was used to calculate the temperature of the thermal storage and to estimate the circulation depth of the karst geothermal water as follows:

$$t=t_0+(H-h)\,r \quad (1)$$

where t is the geothermal reservoir temperature (°C); t_0 is the temperature of the constant temperature belt (°C); r is the geothermal gradient (°C/100 m); h is the depth of the constant temperature belt (m); and H is the maximum circulation depth of the geothermal water (m).

According to the results of the geothermal resource exploration, there are differences in the geothermal gradient in both the horizontal and vertical directions. The difference in the geothermal gradient of the caprock is more obvious, and the shallower the limestone thermal reservoir depth is, the higher the geothermal gradient of the caprock is. According to the borehole temperature measurement data, the geothermal gradient in this area was taken as 2.6°C/100 m. It was calculated that the circulation depth of the Ordovician karst thermal storage geothermal water in the Heze buried uplift area is generally 1785–2690.38 m (Table 4).

Table 4 Calculated karst geothermal water cycle depth in the Heze buried uplift

Sample Location	Well Depth (m)	Geothermal reservoir	Water temperature (°C)	Calculated reservoir temperature (°C)	Maximum hot water circulation depth (m)
HR1	1580.30	Ordovician	54.0	64.34	1856.15
HC1	1500.35	Ordovician	56.0	63.74	1833.07
HJ1	1402.19	Ordovician	53.1	70.57	2095.76
CZ1	1997.98	Ordovician	68.0	86.03	2690.38
JZ1	1436.20	Ordovician	52.0	75.26	2276.15
HN1	1530.00	Ordovician	53.3	73.43	2205.76
HC2	1519.19	Ordovician	53.0	69.13	2040.38
YS1	1810.00	Ordovician	54.04	72.60	2173.84
DQ1	1230.26	Ordovician	58.0	62.49	1785.00

4.2 Characteristics of karst hydrodynamic field

4.2.1 Horizontal flow field characteristics

The karst geothermal water in the Heze buried uplift is deeply buried, and it mainly receives recharge from atmospheric precipitation and infiltration in the mountainous areas in the northeastern and eastern parts of the study area, that is, the Liangshan and Jiaxiang mountainous areas. After being heated through deep circulation, the groundwater flows along the faults, limestone bedding planes, and fractured karst development zone to recharge the karst geothermal water (Figs. 2, 6). Before 2013, The geothermal wells CZ1 was mainly mined for hot spring bathing. In most other areas, the scale of the exploitation of the karst geothermal water was small, and the geothermal water was basically in a natural equilibrium state. According to the existing geothermal well water level monitoring data, the geothermal water flow occurs in two directions: from east to west and from northeast to southwest. After 2013, the exploitation of the geothermal water in the urban areas of Yuncheng, Juancheng, and Heze increased year by year, and a drawdown funnel was formed in the Heze urban area. The water level elevation in the center of the funnel was less than −5 m(figure 7), and the water level was deeper than 54 m, resulting in runoff of the geothermal groundwater toward the center of the funnel. In the urban area of Yuncheng-Juancheng-Heze, the water level drawdown was more than 17 m.

4.2.2 Dynamic characteristics of geothermal water level

According to the dynamic geothermal water level data for the Juancheng, Yuncheng, and Heze urban areas, the dynamics of the karst geothermal water in these areas are affected by factors such as the geological structural conditions, artificial mining, and lateral runoff, and there are great differences in the different regions.

(1) Yuncheng concentrated mining area

The karst geothermal water in Yuncheng is close to the recharge area. There are 51 geothermal wells in total, and the annual production volume is about 3.2 million m^3. With the increase in mining, the level of the geothermal water has exhibited a dynamic decreasing trend. The water level in the geothermal water monitoring well in Yuncheng started to drop from 30.97 m on September 24, 2014, and the water level dropped to 36.03 m at the end of the heating period on March 10, 2015, a total drop of 5.06 m in 4 months. After the heating was stopped, the water level rose slowly. Before the heating in November 2015, it had recovered to 34.18 m, i.e., a recovery of 1.85 m. Compared with the previous year, the water level dropped by 3.21 m. The geothermal water level in this concentrated mining area dropped by 16.22 m in five years, with an average annual decrease of 3.24 m (Fig. 8).

(2) Juancheng concentrated mining area

The karst geothermal water in Juancheng is close to the recharge area. There are 40 geothermal wells in total, and the annual production volume is about 2.53 million m^3. Since November 14, 2014, the burial depth of the water level of the geothermal well began to decrease from 34.75 m, and by the end of the heating period on March 11, 2015, the burial depth of the water level had dropped to 64.45 m, a drop of 29.7 m in 4 months. Before the heating began in November 2015, it had recovered to 37.88 m, i.e., a recovery of 26.57 m. Compared with the previous year, the water level dropped by 3.13 m. From 2014 to 2019, the burial depth of the water level decreased by 3.67 m per year (Fig. 9).

(3) Heze urban concentrated mining area

The karst geothermal water in the Heze urban area is far away from the recharge area. There are 32 geothermal wells in total, with an annual production of about 1.316 million m^3. According to the monitoring data for the geothermal well, from November 2011 to November 2018, the water level decreased by a total of 26.31 m in 7 years, with an average annual decrease of 3.76 m. The water level recovery rate during the non-heating period was significantly smaller (Fig. 10).

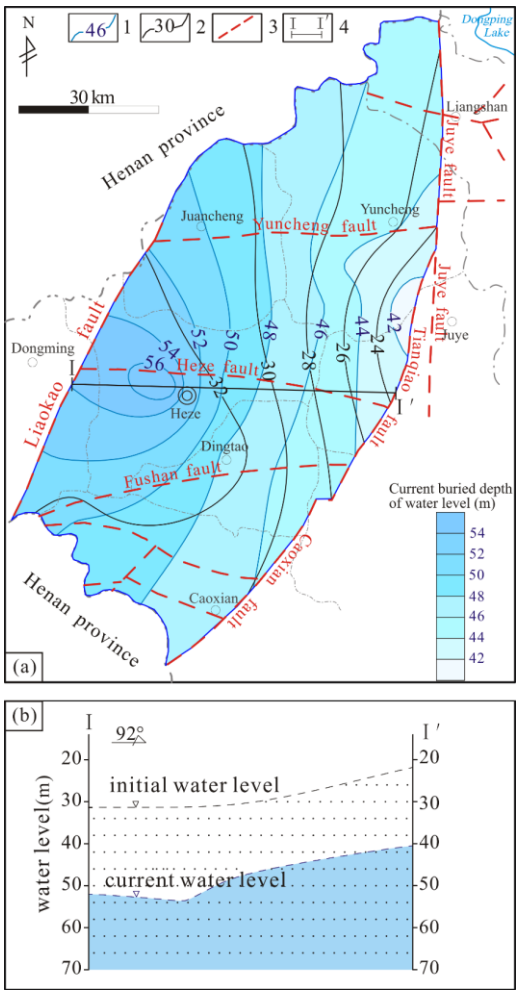

Figure. 6 (a) Initial water level contours and current water level depth zonation of the karst geothermal water in the Heze buried uplift, and (b) the water level profile

1—contours of current water level burial depth (m) (August 2018); 2—contours of initial water level burial depth (m) (August 2013); 3—faults; 4—cross section line

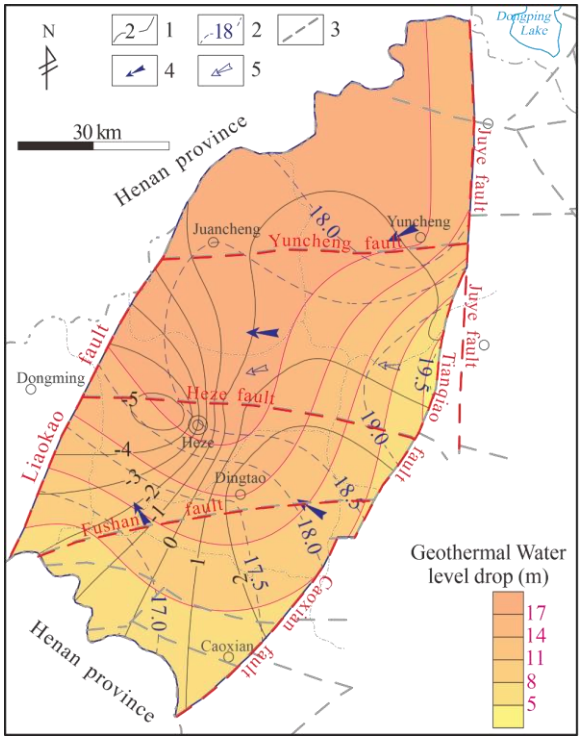

Figure. 7 Geothermal water level drawdown zoning and contours in the karst reservoir in the Heze buried uplift

1—contours of current water level burial depth (m) (August 2018); 2—contours of initial water level burial depth (m) (August 2013); 3—faults; 4—current geothermal water flow directions; 5—initial geothermal water flow directions and faults

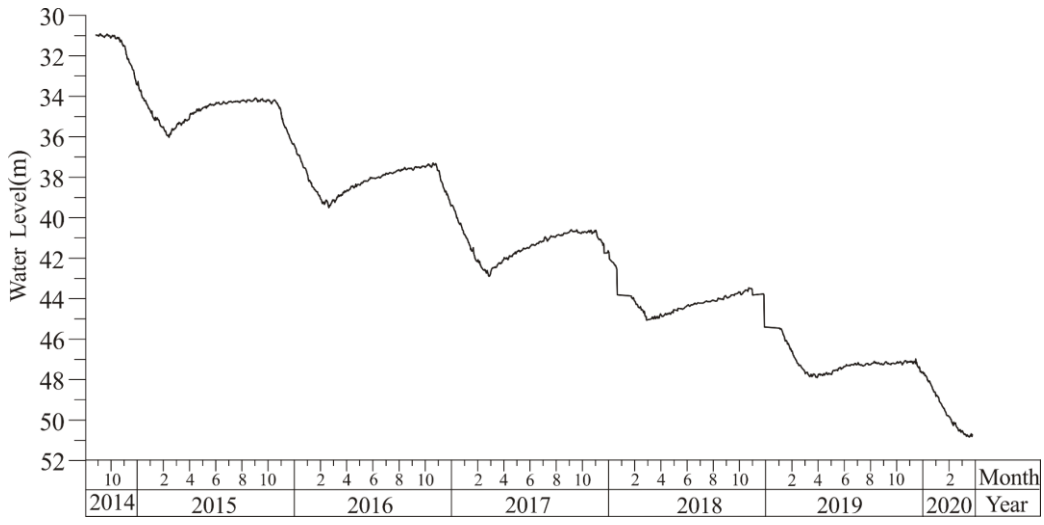

Figure. 8 Dynamic changes in the geothermal water level in the well in Yuncheng from 2014 to 2020

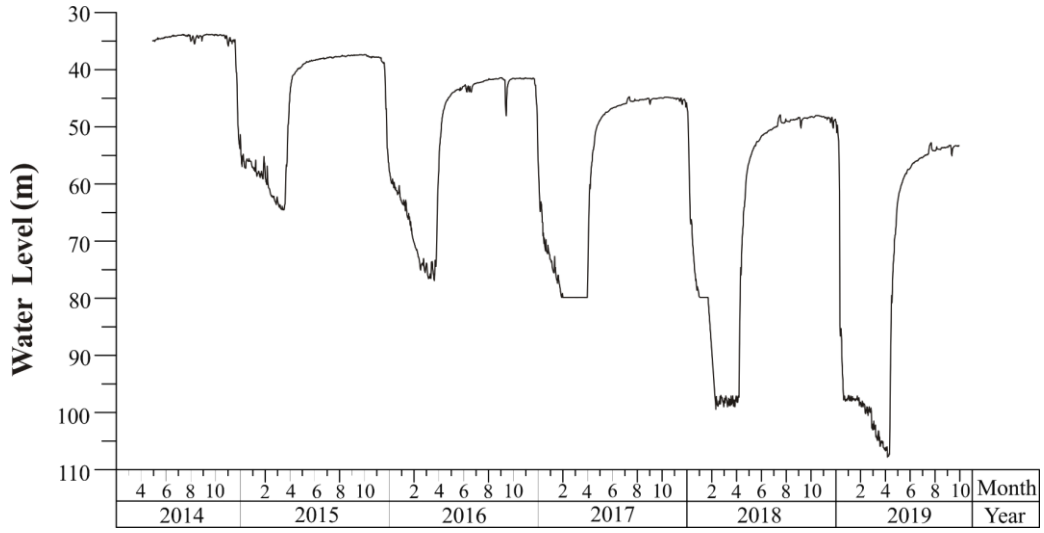

Figure. 9 Dynamic changes in geothermal water levels in Juancheng from 2014 to 2019

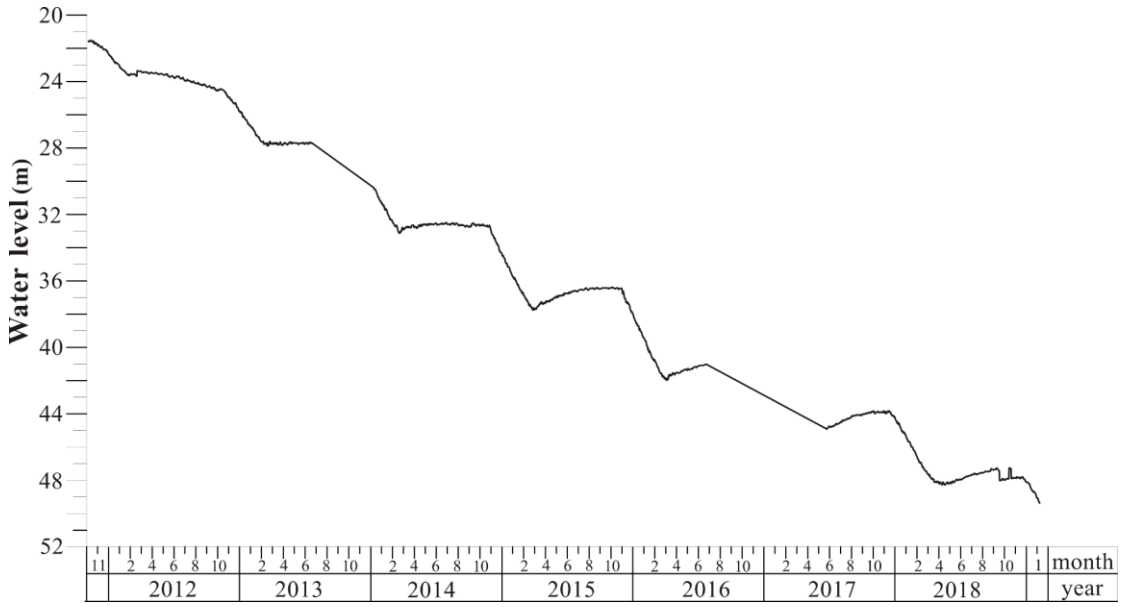

Figure. 10 Dynamic changes in the geothermal water level in Dingtao from 2011 to 2019

4.3 Chemical characteristics of karst water

The Piper diagram of the hydrochemistry of the karst groundwater and geothermal water in the study area is shown in Figure 11. According to the hydrochemical characteristics of the karst geothermal water and the karst cold groundwater, the karst groundwater can be divided into three groups. The first group is the exposed karst rechargeable mountainous areas, i.e., Liangshan in the northeast and Jiaxiang in the east, with shallow circulation-open karst groundwater. The second group is the covering karst area, i.e., the medium circulation-semi-open karst geothermal water in the runoff area in the Juye area. The third group is the deeply buried karst area, i.e., the deep-circulation-weakly open karst geothermal water in the discharge areas in Yuncheng, Juancheng, Heze urban area, Dingtao, and Caoxian Zhuangzhai (Zhu et al., 2005; Chen et al., 2010; Zhang, 2011; Zhao et al., 2017).

The evolution path of the geothermal water from the recharge-runoff-discharge area is as follows. From the shallow circulation-open karst groundwater flow system in the recharge area (I) to the medium circulation-semi-open karst geothermal water flow system in the runoff area (II), to the deep circulation-weakly open karst geothermal water flow system in the discharge and detained area (III), the hydrochemical type gradually evolves from $SO_4 \cdot HCO_3$-Ca·Mg to SO_4-Ca to SO_4-Ca·Na. The total dissolved solids (TDS) gradually increases, and the average value increases from 1064.59 mg/L to 3073.00 mg/L to 3719.52 mg/L. The HCO_3^- content gradually decreases, and the average decreases from 351.04 mg/L to 207.28 mg/L to 198.22 mg/L. The SO_4^{2-}, Cl^-, Ca^{2+}, and Mg^{2+} contents increase gradually. The average concentration of SO_4^{2-} increases from 391.29 mg/L to 1681.90 mg/L to 1814.20 mg/L; the average concentration of Cl^- increases from 159.17 mg/L to 282.73 mg/L to 512.85 mg/L; the average concentration of Ca^{2+} increases from 153.67 mg/L to 490.44 mg/L to 513.68 mg/L; and the average concentration of Mg^{2+} increases from 68.16 mg/L to 114.00 mg/L and 106.75 mg/L. The concentrations of K^+ and Na^+ increases gradually. The average K^+ concentration increases from 3.7 mg/L to 22.18 mg/L to 36.08 mg/L; and the average Na^+ concentration increases from 114.60 mg/L to 242. 26 mg/L to 503.16 mg/L. The evolution path is as follows.

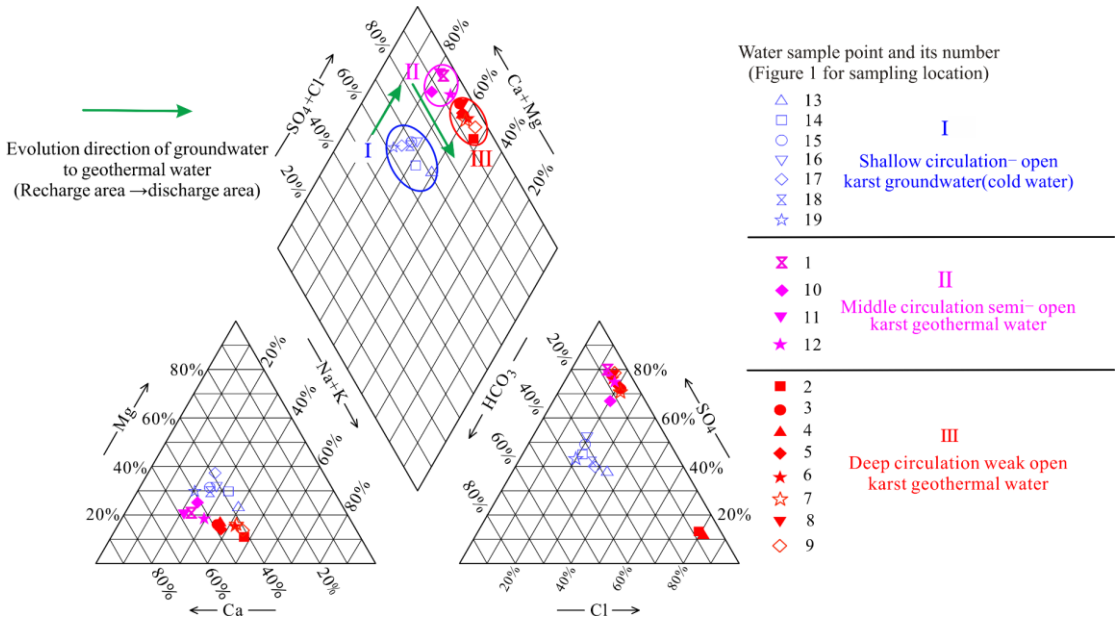

Fig. 11 Piper diagram of the groundwater in the recharge area and the geothermal water in the Heze buried uplift

From the exposed karst rechargeable mountainous areas to the shallow buried karst runoff area in the Juye area to the deeply buried karst discharge areas in Yuncheng, Juancheng, and the Heze urban area, the karst groundwater flows from the shallow-open type system (I), gradually evolves into a medium circulation-semi-open type system (II), and then evolves into a deep circulation-weakly open type system (III), and the water temperature gradually increases from 17°C to 80°C.

The karst groundwater in Zone I has a short runoff path and a shallow circulation depth, and the chemical environment of the groundwater is in an open state. The karst groundwater in Zone II has a long runoff path and a deep circulation depth, and the chemical environment of the karst groundwater is in a weakly-open state, so it can receive the lateral runoff recharge from the karst groundwater in Zone I. The karst groundwater circulation depth in Zone III increases, the distance from the recharge area is farther, and the runoff path is longer. Affected by the water blocking faults, i.e., the Juye fault in the east, the Liaokao fault in the west, and the Changleji fault in the south, the migration speed of the groundwater runoff is slow. The karst groundwater gradually evolves into karst geothermal water, and the hydrochemical environment of the geothermal water is relatively closed. From zone I to zone II to zone III, the hydrochemical environment of the karst groundwater gradually evolves from an open state to a relatively open state to a weakly open state (Fig. 12).

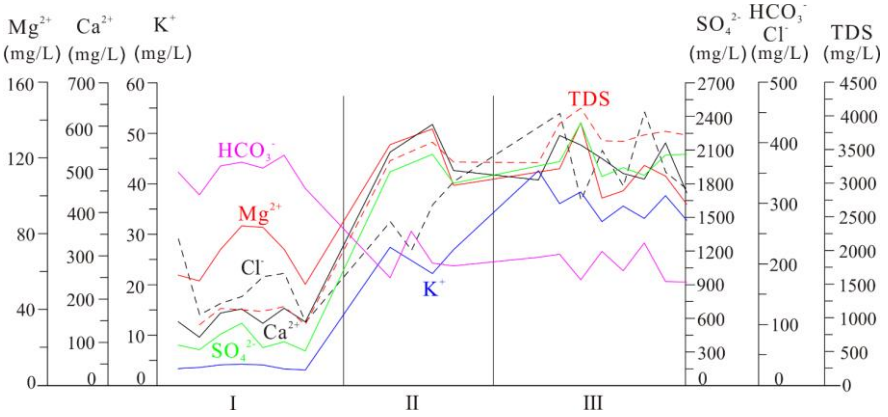

Figure. 12 Variations in the main ion contents in the different zones

4.4 Isotopic characteristics of geothermal water

The hydrogen, oxygen, and ^{14}C isotope characteristics were used to analyze the recharge source of the geothermal water in the Heze buried uplift (Wang et al., 1993; Ma et al., 2006; Su et al., 2007; Zhang et al., 2010; He et al., 2014; Sun et al., 2016). Regarding the hydrogen and oxygen isotope data for the study area (Table 3), the δD value of the geothermal water ranges from −63.92‰ to −80.94‰, with an average of −72.89‰; and the $\delta^{18}O$ value ranges from −6.4‰ to −9.96‰, with an average of −8.24‰. The hydrogen and oxygen isotope data for the geothermal water samples all plot near the Craig standard precipitation line $\delta D=8\delta^{18}O$ (‰) +10 (Fig. 13), indicating that the geothermal water originated from atmospheric precipitation. However, it was not directly from the nearest inflow of local atmospheric precipitation and infiltration recharge. Due to the long distance of the runoff migration, there was significant hydrogen and oxygen isotope drift. For example, geothermal water samples DQ1 and HR1 exhibited obvious positive drift of ^{18}O.

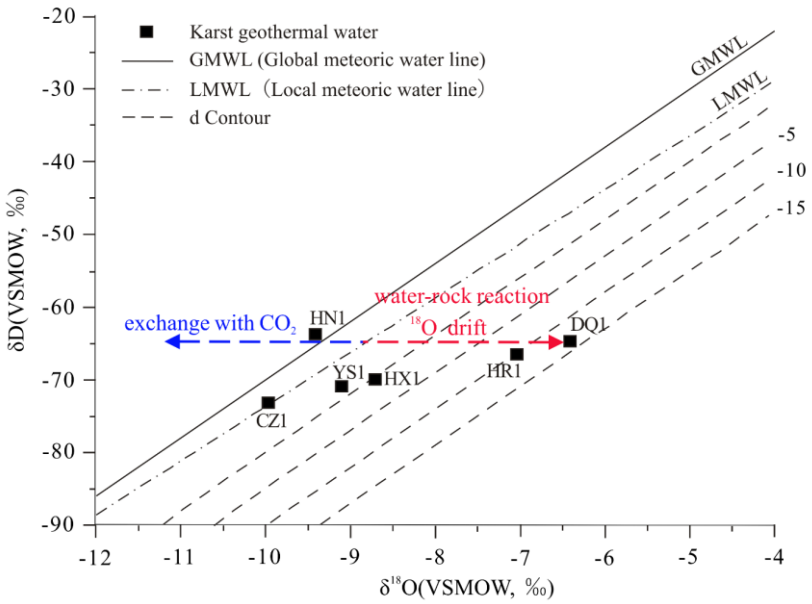

Figure. 13 Plot of δD versus $\delta^{18}O$ for the Heze buried uplift

The ^{14}C ages of the karst geothermal water in the Heze buried uplift area and the corrected ^{14}C ages (Zhou et al., 2003; Guo et al., 2007; Mao et al., 2010) are presented in Table 3, and the ^{14}C corrected age contour division is shown in Figure 14. The ^{14}C corrected age of the karst geothermal water increases gradually from the recharge area to the discharge area. The minimum age occurs in geothermal well UG1 (12.82 ka), and the maximum age occurs in geothermal well HR1 (34.67 ka). This indicates that the further the karst geothermal water is from the recharge area, the worse the circulation renewal ability of the geothermal water is, and the older the age of the water is.

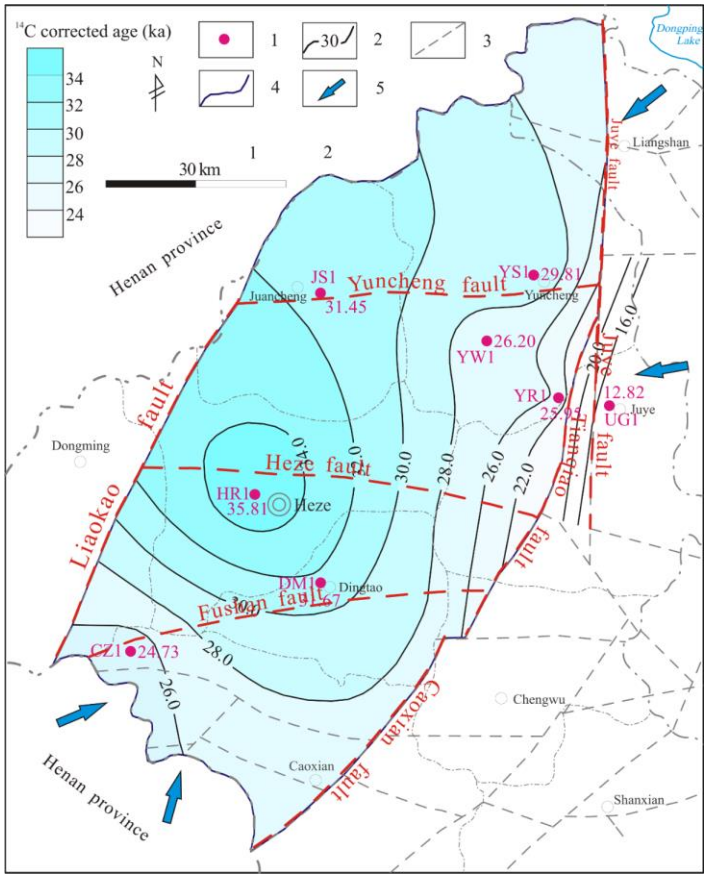

Figure. 14 Corrected ^{14}C age isolines of the karst geothermal water in the Heze buried uplift

1 − Karst geothermal water sampling sites; 2 − contours of ^{14}C corrected ages (ka); 3 − faults; 4 − range of Heze buried uplift; 5 − flow directions of the karst geothermal water

4.5 Distribution of geo-temperature field

According to the temperature measurement data for 24 shallow boreholes and nine geothermal wells, a geo-temperature zonation map at a depth of 30 m and a caprock geothermal gradient zonation map of the Heze buried uplift were drawn, showing the spatial distribution characteristics of the geothermal field in the study area.

4.5.1 Characteristics of horizontal geo-temperature field

The variations in the geothermal temperature in the horizontal direction were mainly related to the tectonically active zone, the recharge conditions of the geothermal water circulation, and the burial depth of the geothermal reservoir. The geothermal value near the active fault zone is larger, while the geothermal value far from the active fault zone is smaller. The geothermal reservoir temperature is lower in the section with better geothermal water runoff conditions, and the geothermal reservoir temperature is higher in the section with poorer geothermal water runoff conditions. The greater the burial depth of the geothermal storage is, the worse the thermal conductivity of the caprock is, and the higher the temperature of the geothermal reservoir is. The shallower the geothermal reservoir is buried, the better the thermal conductivity of the caprock is, and the smaller the geothermal gradient is (Chen et al., 1982). According to the geo-temperature zonation map for a depth of 30 m (Fig. 15), the distribution characteristics of the geothermal field are as follows.

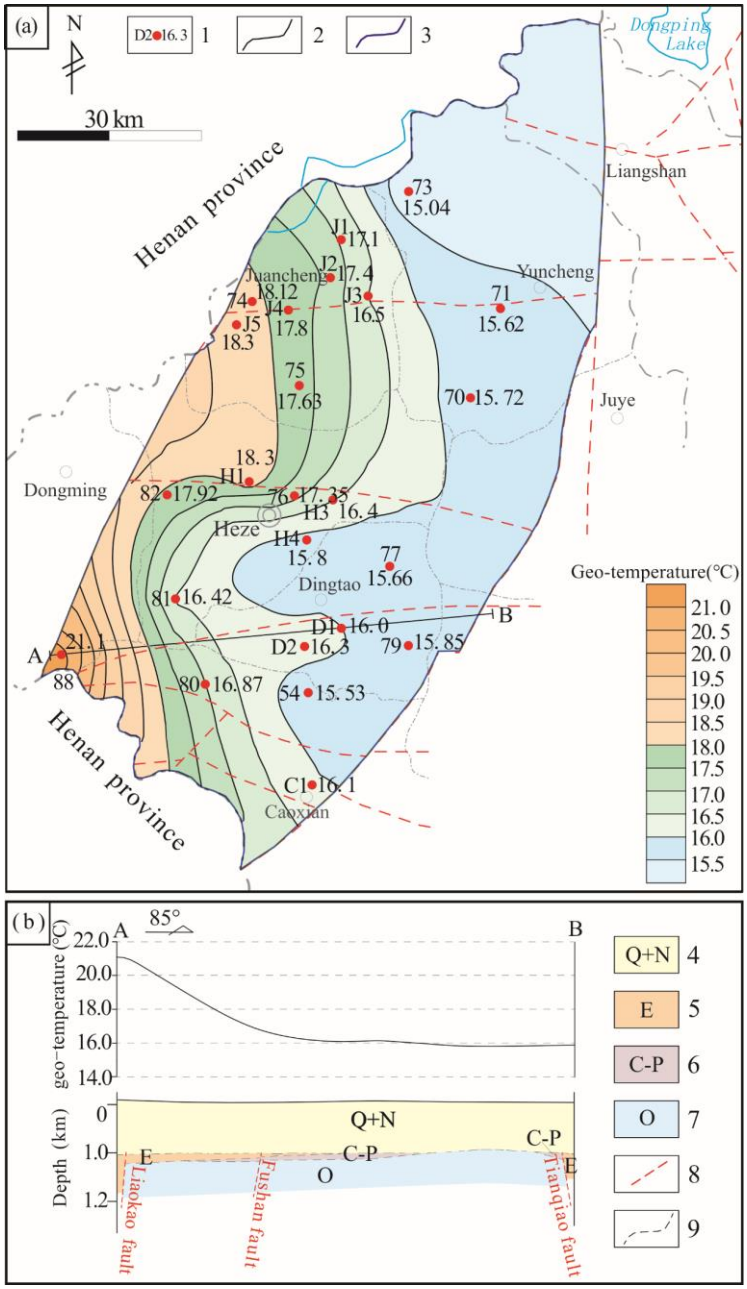

Figure. 15 Geo-temperature zonation and profile at a depth of 30 m in the Heze buried uplift

1—Temperature measuring points and temperature values; 2—geothermal contours; 3—range of Heze buried uplift; 4—Quaternary-Neogene; 5—Paleogene; 6—Carboniferous-Permian; 7-Ordovician; 8-faults; 9—unconformity boundary

(1) The >18°C geo-temperature zone is mainly distributed along the Liaokao fault in a NNE direction. It is close to the regional deep and large thermal-conductivity faults. The geothermal water circulation runoff conditions are poor. The thickness of the caprock is generally greater than 2000 m, and the rock is mainly sandstone and mudstone. The thermal conductivity is poor, and the geo-temperature is greater than 18°C. At the intersection of the Liaokao, Heze, Fushan, Changleji, and other faults, the width of the high temperature zone is large.

(2) The 16–18°C geo-temperature zone is located in the middle of the study area, and exhibits an S-shape in the north-south direction. It is located far away from the Liaokao fault, with good geothermal water circulation and runoff conditions, a caprock thickness of about 1500 m, and geo-temperatures of 16–18°C. The geothermal values close to the Heze and Fushan faults are relatively high, exhibiting an obvious peak value on the geothermal profile.

(3) The <16°C geo-temperature zone is located in Yuncheng and Juye in the eastern part of study area. It is close to the recharge area, with good geothermal water circulation and runoff conditions; and it is located far away from the Liaokao fault zone, with a caprock thickness of about 1000 m and geo-temperatures of less than 16°C.

4.5.2 Characteristics of geothermal gradient

The variations in the geothermal gradient are mainly affected by the structure, lithology, and thickness of the caprock. The general distribution law is as follows. The geothermal gradient is high near the deep and large fault zone, and the geothermal gradient is low in the exposed bedrock recharge area. The geothermal gradient increases gradually from east to west and from north to south. As is shown in Figure 16, in the northeastern part of the study area, Yuncheng and Juye in the eastern part are close to the karst cold water recharge area, where the groundwater runoff is fast and the geothermal gradient is small (1.38 to 1.98°C/100 m). Geothermal wells HN1 and DM1 are located far away from the recharge area and the deep-large water-conducting and heat-conducting faults. The geothermal gradients in these wells are 3.28°C/100 m and 3.29°C/100 m, representing the geothermal gradient for the normal conduction of the geothermal field caprock in the Heze buried uplift. At the intersection of the Liaokao fault and the Fushan fault, the geothermal gradient of the Cenozoic caprock in geothermal well CZ1 is 4.2°C/100 m. The temperature of the Ordovician thermal reservoir is 59.6–75.2°C. The temperature increases by 15.6°C, and the geothermal gradient still reaches 3.1°C/100 m (Fig. 17). This indicates that the deep hot water upwells along the open deep fault zone, resulting in local water-heat convection, and convective heat transfer and conduction heat transfer are superimposed, forming an area with an abnormally high geothermal gradient. The area in which the caprock's geothermal gradient that exceeds pure conduction warming (0.92°C/100 m) is caused by the upwelling of geothermal water in the middle and deep parts of the Cambrian-Ordovician carbonate rocks under the caprock along this fault intersection.

The >18°C geo-temperature zone of is mainly distributed along the Liaokao fault in an NNE direction. It is close to the regional deep and large thermal-conductivity faults. The geothermal water circulation runoff conditions are poor. The thickness of the caprock is generally greater than 2000 m, and the rock is mainly sandstone and mudstone. The thermal conductivity is poor, and the geo-temperature is greater than 18°C. At the intersection of the Liaokao, Heze, Fushan, Changleji, and other faults, the width of the high temperate zone is large.

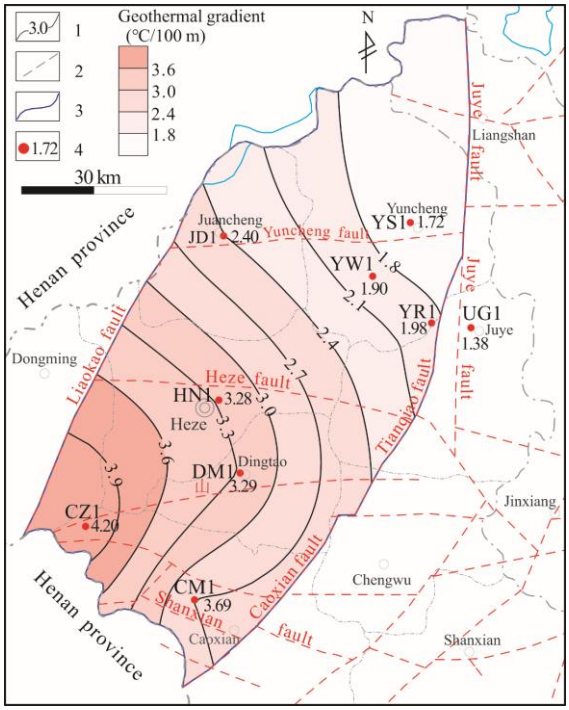

Figure. 16 Zonation map for the geothermal gradient of the cap rock of the karst geothermal reservoir in the Heze buried uplift

1-Geothermal gradient contours (°C/100 m); 2-faults; 3-range of Heze buried uplift; 4-boreholes and their geothermal gradient values (°C/100 m)

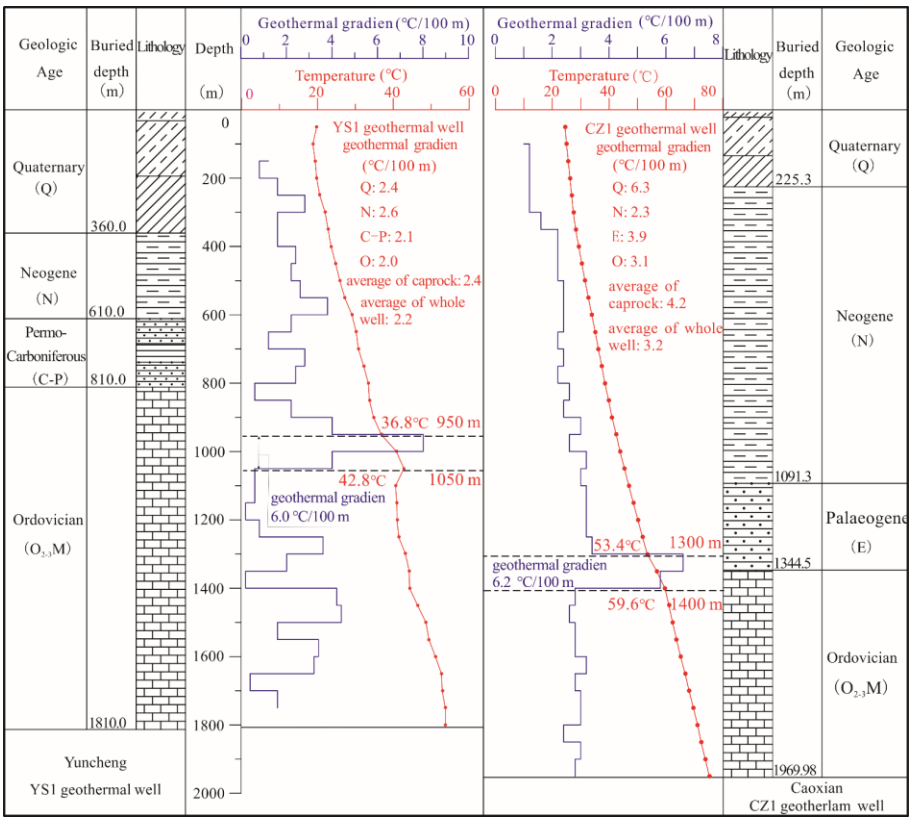

Figure. 17 Comparison of temperature measurements for geothermal wells in Caoxian and Yuncheng, i.e., near and far away from the Liaokao fault

Wells CZ1 and YS1 are overshoot sections in terms of the geothermal gradient at the interface between the caprock and the Ordovician karst thermal reservoir, and the geothermal gradient is as high as 6.0°C/100 m and 6.2°C/100 m in these wells. This is mainly because the Ordovician limestone and dolomite have compact structures and high thermal conductivities, reaching 3–5 W/(m·K). In contrast, the overlying Cenozoic sandstone and mudstone have loose structures and low thermal conductivities, with an average value of 1.97 W/(m·K) (Clauser et al., 1995; Gong et al., 2003; Hu et al., 2015; Jiang et al., 2016), which is only 50% that of the Ordovician limestone and dolomite. Correspondingly, the thermal resistance value of the Cenozoic sandstone and mudstone is double that of the Ordovician limestone and dolomite, resulting in the heat flow in the geothermal reservoir encountering a high thermal conductivity encountering resistance in the upward transfer process into the caprock and gathering in the zone where the top of the geothermal reservoir and the bottom of the caprock meet. This causes the geothermal gradient to increase significantly. After entering the Ordovician geothermal reservoir, the geothermal fluid activity becomes strong, and the geothermal gradient decreases significantly due to the influence of water-heat convection. However, the geothermal gradient is still 3.1°C/100 m in well CZ1, which is 1–2°C/100 m higher than in the geothermal wells far away from the deep and large thermal conductivity faults.

5. DISCUSSION

5.1 Geothermal water cycle enrichment mechanism

The main recharge source of the karst geothermal water in the geothermal field in the Heze buried uplift is the deep circulation runoff of groundwater formed via the infiltration of atmospheric precipitation in the bedrock mountainous areas in Liangshan and Jiaxiang. It is a weakly open karst reservoir geothermal field. In the water-conducting fault zone and the interlayer karst development zone, fissured karst has developed, forming a strong groundwater runoff zone, which provides space for the storage and circulation of geothermal water, forming a geothermal water enrichment area. In particular, in the composite position of the fault structure, the structural karst, interlayer karst, fissures, dissolved pores, and karst caves are more developed, forming strong fractured karst development belts, which serve as strong permeability dominant water-conducting channels. These channels gather the geothermal water from a wide area into the layered geothermal reservoir, and the hot water gathers into those dominant water-conducting channels to form a water enrichment zone with strong geothermal water runoff. In this zone, the karst fissure rate, permeability coefficient, and water conductivity coefficient can be one to three orders of magnitude higher than in the surrounding rocks. Therefore, the water-conducting fault zone and the interlayer karst composite site are the enrichment zone of the geothermal water circulation.

5.2 Thermal accumulation from four sources

Based on analysis of the geological structure, lithology, lateral runoff and vertical migration of groundwater, caprock thickness, and spatial distribution characteristics of the geo-temperature field in the Heze buried uplift, the heat source mechanism of the geothermal field was determined. In addition, a four-source heat accumulation mechanism is proposed for the weakly-open karst heat storage (Kang et al., 2020). The first source is the thermal accumulation of the blanket-shaped terrestrial heat flow. The second source is the thermal accumulation caused by the high thermal conductivity difference in the uplift area. The third source is the belt-shaped convective thermal accumulation in the deep fault zone and the contact zone between the intrusive and soluble rocks. The fourth source is the conductive and convective thermal accumulation through the deep groundwater circulation.

(1) The thermal accumulation of the blanket-shaped terrestrial heat flow: The terrestrial heat flow is the heat transferred from the interior of the Earth to the surface, and the comprehensive quantitative characterization of the thermal state in the deep crust or lithosphere is reflected on the surface. There is a huge amount of heat energy inside the Earth, and it is continuously released. The Moho surface of the geothermal field in the Heze buried uplift has a burial depth of 34–39 km. The value of the terrestrial heat flow in the Heze buried uplift is 70–90 mW/m^2 greater than that in northern China, i.e., 1.47±0.32 HFU (61.55±13.40 mW/m^2) (Chen, 1988; Kang, 2018). The areas close to the east side of the Liaokao fault and the mantle uplift area in the urban area in Yuncheng County are favorable positions for geothermal formation. In these areas, the terrestrial heat flow is 80–90 mW/m^2, and the blanket-shaped heat conduction accumulation of the terrestrial heat flow is the main heat source in this area.

(2) The thermal accumulation of the high thermal conductivity difference in the uplift area: The thermal conductivity of the Ordovician limestone in the uplift area is high, with an average value of 3.53 W/(m·K) and a maximum value of 4.95 W/(m·K), and the thermal conductivity is fast. The sandstone and mudstone in the depression area on both sides have a low thermal conductivity, with an average value of 1.97 W/(m·K), and a high thermal resistance. When the terrestrial heat flow is conducted upward, it is affected by the difference in the thermal conductivities of the crustal rocks, so the more uniform heat flow from the deep part is redistributed in the shallow part of the crust, and the heat flow accumulates in the rocks in the bulge area, which has a high thermal conductivity.

(3) Convective heat accumulation via the high thermal conductivity faults: The deep and large faults in the study area, such as the Liaokao, Tianqiao, and Wensi faults, connect the deep crust and even the upper mantle with the shallow geothermal fluid and heat flow.

(4) Conductive and convective thermal accumulation through deep groundwater circulation: The groundwater in the study area flows from Liangshan and Jiaxiang to the runoff area around Yuncheng and Juye and the discharge areas such as the Heze urban area and Juancheng county urban area. The groundwater migrates through long-distance deep circulation, continuously absorbing the heat from the surrounding rocks through heat conduction. This heats the groundwater, turning it into geothermal water in the deep area. The geothermal water transfers the heat in the water medium through thermal convection as it upwells, and heats the groundwater along its path, turning it into geothermal water.

5.3 Genetic mechanism of the Heze buried uplift geothermal field

Geothermal fields can be divided into different types according to the single element factor controlling the geothermal resources. Taking the thermal reservoir as a single element, based on the spatial morphological characteristics and type of medium of the thermal reservoir, geothermal fields can be divided into cavity type, belted-layered composite type, and layered type geothermal fields. Taking the water source as a single element, based on the recharge, runoff, discharge, and enrichment of the geothermal fluid, geothermal fields can be divided into open, weakly open, and closed geothermal fields. Taking the heat source as a single element, based on the heat source of the geothermal fluid and its upwelling channel and heat transfer mode, geothermal fields can be divided into convection, convective-conduction composite, and conduction geothermal fields.

The Heze buried uplift geothermal field is mainly a layered karst reservoir, and its interlayer karst is well-developed. At the intersection with the structural fracture karst development zone, the geothermal reservoir is mainly layered and belt-shaped, making it a belted-layered type reservoir. The main recharge source of the geothermal water is the deep circulation runoff recharge of the groundwater formed via the infiltration of atmospheric precipitation in the bedrock mountainous areas in Liangshan and Jiaxiang. It is enriched at the intersection of the structural fissured karst and interlayer karst and is a weakly open karst thermal reservoir geothermal field. According to the heat sources and transfer and accumulation characteristics, the karst reservoir heat source is dominated by surface source conduction and accumulation, which is supplemented by local belted convection and accumulation, so it is a conduction-convection composite type reservoir in terms of heat accumulation.

The genetic model of the karst reservoir geothermal field in the Heze buried uplift is as a weakly open, convection-conductive, belted-layered type, which comprehensively considers the main ore-controlling factors of the geothermal resources such as the water source, heat source, and thermal reservoir space. The metallogenic model reveals the renewable capacity of the karst reservoir's geothermal water source and its enrichment, the heat source and its transfer and accumulation, and the regularity of the spatial occurrence of the thermal reservoirs in the buried uplift in this sedimentary basin. This provides a basis for the exploration and exploitation of the geothermal resources.

6. CONCLUSIONS

(1) The karst geothermal reservoir in the buried uplift geothermal field in the sedimentary basin is distributed in layers, and interlayer karst is developed. At the intersection with the structural fractured karst development zone, the reservoir is mainly layered and belt-shaped, making it a belted-layered type reservoir.

(2) The main recharge source of the karst geothermal water is the deep circulation runoff of the groundwater formed via the infiltration of atmospheric precipitation in the bedrock mountain areas. The karst geothermal water is enriched at the intersection of the structural fissure karst and interlayer karst, and it is a weakly open karst thermal storage geothermal field.

(3) A four-source heat accumulation mechanism is proposed for this geothermal reservoir. The first source is the thermal accumulation of blanket-shaped terrestrial heat flow conduction. The second source is the thermal accumulation caused by the high thermal conductivity difference in the uplift area. The third source is the belt-shaped convective thermal accumulation in the deep fault zone and the contact zone between the intrusive and soluble rocks. The fourth source is the conductive and convective thermal accumulation through deep groundwater circulation. The area where these four sources all occur has the largest heat flow density and the highest geothermal gradient, which is the heat flow accumulation area.

(4) Based on the characteristics of the genetic elements of the geothermal resources, such as the thermal reservoirs, water sources, and heat sources, the metallogenic model of the karst reservoir geothermal field in the buried uplift in the sedimentary basin is categorized as a weakly open, convective and conduction, belted-layered geothermal resource. This metallogenic model reveals the renewability and enrichment of the karst reservoir's geothermal water sources in the buried uplift in the sedimentary basin, the heat sources and their transfer and accumulation, and the regularity of the spatial distribution of the reservoir. This provides a basis for geothermal resource exploration and exploitation.

(5) In the sedimentary basin, the intersection of the interlayer karst and structural fracture karst development areas in the karst groundwater deep circulation retention area is not only the four-source heat flow accumulation zone but is also a geothermal water enrichment zone. Furthermore, it is the main target area of the heat flow concentration area.

ACKNOWLEDGEMENT

This research was financially supported by the National Natural Science Foundation of China (grant numbers 42072331, U1906209) and Taishan Scholar Foundation. We are grateful to editors and reviewers for their constructive comments and valuable suggestions that significantly improved this manuscript.

REFERENCES

Axelsson G.2008.Production capacity of geothermal systems// Workshop or Decision Makers on Direct Heating Use of Geothermal Resources in Asia.

Chang Jian, Qiu Nansheng,Zhao Xianzheng et al.2016. Present-day geothermal regime of the Jizhong Depression in Bohai Bay Basin,East China. Chinese Journal of Geophysics, 59(3):1003-1016(in Chinese).

Chen Moxiang, Huang Geshan,Zhang Wenren,Zheng Rongyan. 1982.The temperature distribution pattern and the utilization of geothermal water at niutuozhen basement protrusion of central hebei province.Scientia Geologica Sinica,(3):239 ~ 252(in Chinese with English abstract).

Chen Moxiang, Deng Xiang, Wang Jun, Wang Jiyang. 1985. Formation Conditions and Occurrence Characteristics of Underground Hot Water in North China Plain. earth science:10(1):83~89(in Chinese).

Chen Moxiang, Wang Jiyang,Wang Ji´an, et al.1990.The characteristics of the geothermal field and its formation mechanism in the north china down-faulted basin. Acta Geologica Sinica, (01):80 ~ 91(in Chinese).

Chen Moxinag, Zhou Mingjian.1988.Geothermal of North China.Beijing:Science Press,85 ~ 117(in Chinese).

Chen Zongyu,Qi Jixiang,Zhang Zhaoji.2010. Application of isotope hydrogeology method in typical basins of North China.Beijing:Science Press,20 ~ 21(in Chinese).

Clauser Christoph and Huenges Erns. 1995. Thermal conductivity of rocks and minerals Rock Physics and Phase Relations. In: A Handbook of Physical Constants: 105 ~ 26.

Dai Minggang,Lei Haifei,Hu Jiaguo,et al.2019.Evaluation of recoverable geothermal resources and development parameters of Mesoproterozoic thermal reservoir with the top surface depth of 3500 m and shallow in Xiong' an New Area. Acta Geologica Sinica, 93(011):2874-2888(in Chinese with English abstract).

Gong Yuchao, Wang Liangshu, Liu Shaowen, et al. 2003. Characteristics of terrestrial heat flow distribution in Jiyang depression [J]. Science in China, 33(4):384 ~ 391(in Chinese).

Guo Jiao,Shi Jiansheng,Wang Wei.2007.Age correction of the groundwater in north china plain.Acta Geoscientica Sinica,28(4):396 ~ 404(in Chinese with English abstract).

He Dan,Ma Zhiyuan,Wang Jiangxia，Zheng Lei.2014.Isotopic evidence fo remaining sedimentary water in the deep geothermal water of guanzhong basin.Journal of Earth Sciences and Environment,36(04):117 ~ 126(in Chinese with English abstract).

Hu Shengbiao and Huang Shaopeng. 2015. Terrestrial heat flow in China. In: Wang Jiyang et al. Geothermics and its applications. Beijing, Science Press: 64 ~ 122(in Chinese).

Jiang Guangzheng,Tang Xiaoyin,Rao Song,Gao Peng,Zhang Linyou, Zhao Ping, Hu Shengbiao. 2016. High-quality heat flow determination from the crystalline basement of the south-east margin of North China Craton. Journal of Asian Earth Sciences, 118 (2016) 1 ~ 10.

Jiang Guosheng.2014.The research on the main factors of controlling the development of Ordovician geothermal reservoirs in Tianjin.Master of Engineering Degree of China University of Geosciences(beijing) (in Chinese).

Kang Fengxin.2018.Assessment of Geothermal Resources in Shandong Province.Beijing:Science Press,14 ~ 93(in Chinese).

Kang Fengxin,Sui Haibo,Zheng Tingting.2020.Heat accumulation and water enrichment mechanism of piedmont karstic geothermal reservoirs:a case study of northern Jinan.Acta Geologica Sinica,94(5):1606~1624.

Li Yi Ming.2019.Characteristics and resource evaluation of geothermal resources in Zhaoxing Town, Luobei County, Heilongjiang Province.Master dissertation of Ji Lin University (in Chinese).

Lin G, Nunn J, Deming D.Thermal buffeting of sedimentary basins by basement rocks: implications arising from numerical simulations[J]. PETROLEUM GEOSCIENCE, 2000, 6(4):299---307.

Liu S, Wang L, Gong Y, et al. Thermal-rheological structure of the lithosphere beneath Jiyang Depression: Its implications for geodynamics[J]. ence in China, 2005, 48(10):1569-1584.

Lu Luo, Zhonghe Pang, Jinxia Liu.etc.2017.Determining the recharge sources and ciriculation depth of thermal waters in Xianyang geothermal field in GuanZhong Basin: The controlling role of Weibei Fault. Geoihennics.55-64.

Mao Xumei,Liang Xing,Wang Fenglin,Han qingzhi. 2010. Calibrating deep groundwater 14C ages of north china plain with TDIC and a comparative study.Earth Science Frontiers,17（6）： 102 ~ 109(in Chinese with English abstract).

Megel T and Rybach L.2000.Production Capacity and Sustainability of Geothermal Doublest Proceedings of the World Geothermal Congress. Kyushu-Tohoku. Japan.849-854.

Muffler L J P. 1979. Assessment of geothermal resources of the United States—1978. Center for Integrated Data Analytics Wisconsin Science Center, 156~162.

Pang Zhonghe, Hu Shengbiao, Wang Shejiao, et al. 2015. Geothermal system and geothermal resources. In: Wang Jiyang, et al., eds. Geothermal Science and Its Application. Beijing: Science Press, 257~376 (in Chinese with English abstract).

Pritchett J W.1998. Modeling post-abandonment electrical capacity recovery for a two-phase geothermal reservoir. Transactions Geothermal Resources Council, 22:521-528.

Rybach L, Muffler L J P. 1981. Geothermal systems: Principles and case histories. New York: John Wiley, 3~76.

Su Yan,Ma Zhi-yuan,Liu Fang,et al.2007.Deuterium excess parameter features study on thermal groundwater of Xi′an and Xianyang. Coal Geology&Exploration,35(3):39-41.

Sun Z , Ma R , Wang Y.2016.Using isotopic, hydrogeochemical-tracer and temperature data to characterize recharge and flow paths in a complex karst groundwater flow system in northern China. Hydrogeology Journal,24(6): 1393 ~ 1412.

Wang Guiling,Lin Wenjing.2020.Main hydro-geothermal systems and their genetic models in China.Acta Geologica Sinica,94(7): 1923 ~ 1937.

Wang Guiling, Zhang Wei, Lin Wenjing, Liu Feng, Zhu Xi, Liu Yanguang, Li jun. 2017. Research on formation mode and development potential of geothermal resources in Beijing-Tianjin-Hebei region[J]. Geology in China, 44(6):1074-1085 (in Chinese with English abstract).

Wang Jiyang,Xiong Liangping,Pang Zhonghe.1990. Using geothermal data to determine the depth of geothermal water circulation.Chinese Science Bulletin,35(5): 378 ~ 380(in Chinese with English abstract).

Wang Jiyang,Xiong Liangping,Pang Zhonghe.1993. Medium and low temperature convective geothermal system. Beijing:Science Press,48 ~ 55(in Chinese with English abstract).

Wright.P.M.The Sustainability of Production from Geothermal Resources. Proceed World Geothermal Congress. Florence. Italy. 18-31 May. 1995.

Zhi-Yuan M A , Ji-Jiao F , Yan S U , et al.2006. Hydrogeology Significance on Hydrogen and Oxygen Lsotopes Composition in Underground Thermal Water of Guanzhong Area,Shaanxi Province. Journal of Earth ences and Environment.

Zhou Tingqiang,Lin Jianwang,Gao Baozhu，Wang Xinyi.2003. Application of radioisotope 14C to geothermal analysis.Journal of Jiaozuo Institute of Technology (Natural Science),22(3):176 ~ 179(in Chinese with English abstract).

Zhu Minghe,Fu Zhong, Liu Yanbing.2005. A discussion on the supply source of underground hot water in the Kaifeng geothermal field based on geochemical methods. ceophysical＆geochemical exploration, 29(6):493 ~ 496(in Chinese with English abstract).

Zhang Baojian,Xu Junxiang,Ma Zhenmin，Shen Zhaoli,Qi Lin.2010. Analysis on groundwater supply sources using hydrogen and oxygen isotopedata — a case study of Yanggu-Qihe salient, northwestern Shandong, China. Geological Bulletin of China,29(4):603 ~ 609(in Chinese with English abstract).

Zhang Baojian.2011.Hydogeochemical characteristics and forming conditions of underground geothermal water in Northwest Shandong Province.doctoral dissertation of China University of Geosciences(Beijing)(in Chinese).

Zhao Xianzheng,Li Fei,Zeng Jianhui,Jin Fengming, Zhang Wangming,Liu Jia,Zhang Jiwei.2017.The geochemical characteristics and origin of deep geothermal water in Baxian Sag.Earth Science Frontiers,24(3):211 ~ 218(in Chinese with English abstract).